Acta Oceanol. Sin., 2018, Vol. 37, No. 11, P. 104–115
DOI: 10.1007/s13131-018-1256-7
http://www.hyxb.org.cn
E-mail: hyxbe@263.net

Application of computational fluid dynamics simulation for submarine oil spill

YANG Zhenglong[1, 2], YU Jianxing[1, 2], LI Zhigan[1, 3, 4], CHEN Haicheng[1, 2], JIANG Meirong[1, 3, 4*], CHEN Xi[1, 2]

[1] State Key Laboratory of Hydraulic Engineering Simulation and Safety, School of Civil Engineering, Tianjin University, Tianjin 300072, China

[2] Collaborative Innovation Center for Advanced Ship and Deep-Sea Exploration, Shanghai 200240 , China

[3] Offshore Oil Engineering Co. Ltd., China National Offshore Oil Corporation (CNOOC), Tianjin 300451, China

[4] CNOOC Research Institute Co. Ltd., China National Offshore Oil Corporation (CNOOC), Beijing 100028,China

Received 24 November 2017; accepted 13 April 2018

Abstract

Computational fluid dynamics (CFD) codes are being increasingly used in the simulation of submarine oil spills. This study focuses on the process of oil spills, from damaged submarine pipes, to the sea surface, using numerical models. The underwater oil spill model is developed, and a description of the governing equations is proposed, along with modifications required for the particalization of the control volume. Available experimental data were introduced to evaluate the validity of the CFD predictions, the results of which proved to be in good agreement with the experimental data. The effects of oil leak rate, leak diameter, current velocity, and oil density are investigated, by the validated CFD model, to estimate the undersea leakage time, the lateral migration distance, and surface diffusion range when the oil reaches the sea surface. Results indicate that the leakage time and lateral migration distance increase with decreasing leak rates and leak diameter, and increase with increasing current velocity and oil density. On the other hand, a large leak diameter, high density, high leak rate, or fast currents result in a greater surface diffusion range. The findings and analysis presented here will provide practical predictions of oil spills, and guidance for emergency rescues.

Key words: oil spill, computational fluid dynamics (CFD), oil particles, current velocity

Citation: Yang Zhenglong, Yu Jianxing, Li Zhigan, Chen Haicheng, Jiang Meirong, Chen Xi. 2018. Application of computational fluid dynamics simulation for submarine oil spill. Acta Oceanologica Sinica, 37(11): 104–115, doi: 10.1007/s13131-018-1256-7

1 Introduction

Oil spills typically occur in submarine pipelines because of corrosion, submarine landslides, ice issues, and ship anchors, resulting in significant damage and destruction to the economy, marine environment, and human health (Wang et al., 2013; Deng et al., 2013). The accidental marine oil leakages in the Gulf of Mexico (Tangley, 2010; Boufadel et al., 2014), and the Penglai 19-3 oilfield in the Bohai Sea (Xu et al., 2013; Yang et al., 2017), released significant amounts of oil into the sea, causing ongoing concern from the associated environmental and social hazards.

In order to reduce the environmental and social consequences, oil leakages require emergency responses, contingency planning, and impact assessments (Zheng et al., 2010). Therefore, predictive information about oil spills is essential. The bulk of previous oil spill models focused on the surface, or near-surface, spills based on environmental input parameters from atmospheric, ocean, and wave forecast models or observations. As reviewed by ASCE Task Committee on Modeling of Oil Spills (1996), Hackett et al. (2009), Marta-Almeida et al. (2013), and Spaulding (2017), such models included OSPM (oil spill process model), OSCAR (oil spill contingency and response), and OD3D (oil drift three-dimensional model). However, for submarine oil spills information such as the submarine trajectory and the migration of spilled oil in the horizontal direction, is also of great importance in providing guidance for emergency rescues (Zhu et al., 2014). Therefore, a fast and accurate prediction model for simulating submarine oil spills could satisfy the above requirements.

Certain scholars have been successful in simulating the process of submarine oil spills, using computational fluid dynamics (CFD) software. Li et al. (2013) simulated the submarine oil spill with current and wave, using FLUENT. Zhu et al. (2014) employed CFD software to simulate the process of oil spilling from a submarine pipeline to the free surface, under a shear current. Jiang et al. (2016) investigated the effect of grid density on the numerical results for oil leakages from a subsea pipeline. Zhu et al. (2017) studied the underwater spreading and surface drifting of oil spilled from a submarine pipeline under the combined action of waves and currents using CFD software. However, the CFD software simulation process requires a greater computation time than the oil-spill mathematical model. Therefore, the mathematical model is more suitable for the early emergency response to unexpected oil spills.

For CFD mathematical models, early studies were primarily

Foundation item: The National Basic Research Program (973 Program) under contract No. 2014CB046803; the National Natural Science Foundation of China under contract No. 51239008; the National Science and Technology Major Project under contract No. 2016ZX05028005-004.

*Corresponding author, E-mail: meirongjiang@live.cn

concerned with the submerged oil jets/plumes in shallow water, such as McDougall (1978), Fannelop and Sjoen (1980), Milgram (1983), Fanneløp et al. (1991), Yapa and Zheng (1997), and Yapa et al. (1999). In order to improve on the inadequacies of Yapa and Zheng's (1997) model for simulating the special behavior of gas in a deepwater environment, an enhanced comprehensive model-ADMS/CDOG was developed by Zheng et al. (2003). Another model in common use is DeepBlow, developed by Johansen (2000). Yapa et al. (2012) studied the general behavior of an oil spill in deepwater, using a model, CDOG, developed by Zheng et al. (2003). Chen et al. (2015) simulated a hypothetical oil spill taking place at the seabed of a deepwater oil/gas field in the South China Sea, using a numerical model based on the previous studies of other scholars. Recent developments in underwater oil spill modeling were summarized by Zhang et al. (2016) and Paiva et al. (2017).

Under the action of currents, the leakage time, lateral migration distance, and surface diffusion range are the three critical parameters that guide oil spill response (Dasanayaka and Yapa, 2009; Chen et al., 2015). Therefore, the understanding of the underwater oil spill process must be as detailed as possible. Figure 1 shows the continuous process of an underwater oil spill. Initially, spilled oil rises as a jet/plume, gradually losing momentum and buoyancy because of the entrainment of the stratified ambient fluid, i.e., the plume-dynamic stage. Above the terminal level of plume dynamics (TLPD), the plume dynamics becomes negligible, and the oil moves as individual droplets because of their non-miscible characteristics, as has been observed in field experiments (Rye et al., 1996; Rye and Brandvik, 1997; Johansen, 2003; Brandvik et al., 2013), i.e., the advection-diffusion stage. The bulk of previous mathematical models (Rye, 1994; Yapa and Zheng, 1997; Zheng et al., 2003; Chen et al., 2015) used the neutral buoyancy level as the TLPD, that enabled simulations on the fate of oil that originated as jets/plumes. However, according to Dasanayaka and Yapa (2009), it was a possibility that, for slow leaks from pipelines or wellheads, the plume-dynamic stage was comparatively short-lived, or non-existent, and that oil initially moves as individual droplets, not plume. Their study also proposed that the droplet buoyant velocity, V_b, corresponding to the median oil droplet size based on volume, can be used as the transition point for TLPD.

In this study, the model by Yapa and Zheng (1997) is improved as follows. The plume-dynamics model (PDM), used to simulate the jet/plume stage, is combined with an advection-diffusion model (ADM) for simulating the advection-diffusion stage; the particalization of the control volume is conducted so that comprehensive, and successive, simulations on oil spill fate can be performed. The droplet buoyant velocity criterion proposed by Dasanayaka and Yapa (2009), is chosen to define the transition point between the PDM and the ADM. A comparison of the improved model, against a selection of experimental data, is then carried out for model verification. The experimental data include oil slow-discharges in un-stratified flowing ambient, and buoyant jets in stratified/un-stratified ambient. In the simulations presented in this study, the turning coefficients did not change from one simulation to another.

Therefore, this study presents and verifies a slightly modified CFD model for simulating submarine oil spills accurately, and is organized as follows. In Section 2, the mathematical models and modifications thereof are presented; Section 3 validates the models by comparing them with available experimental data; Section 4 presents the numerical results of a parametric study and a discussion of the results; the concluding remarks are presented in Section 5.

2 Mathematical model

According to the actual scenario of an oil spill, the present model comprises two sub-models: the PDM is used to simulate the jet/plume stage, while the ADM is used to simulate the ad-

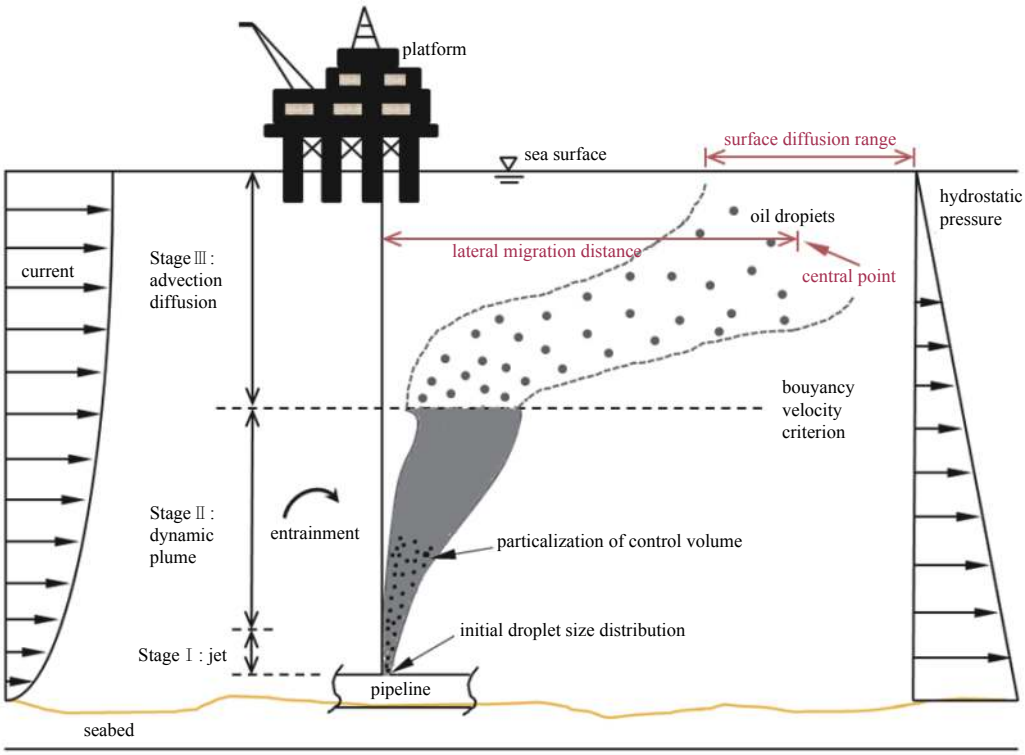

Fig. 1. Underwater oil spill process.

vection-diffusion stage.

2.1 *Plume-dynamics model (PDM)*

The plume-dynamics model was developed, based on the Lagrangian integral control volume (CV) method proposed by Yapa and Zheng (1997). Some modifications were implemented to improve the applicability for simulating crude oil droplets accurately, without gas bubbles, such as particalization of the CV (Fig. 1). In this model, the CV element moves with its local velocity along the centerline of the buoyant plume. Therefore, the CV element height is $h=\left|\vec{V}\right|\Delta t$, where $\left|\vec{V}\right|$ is the local velocity, and Δt is time step. The element mass is $m=\rho\pi b^2 h$, where ρ and b are the density and radius of the buoyant jet/plume, respectively. Based on Lee and Cheung's study (1990), $\Delta t=0.1b_0/\left|\vec{V}\right|$, where b_0 is the initial radius. The following governing equations are applied to the CV.

2.1.1 *Mass conservation equation*

Conservation of the oil mass in the CV is written as (Yapa and Zheng, 1997):

$$\frac{\mathrm{d}m}{\mathrm{d}t}=\rho_\mathrm{a}Q_\mathrm{e}-\sum_i^n\frac{\mathrm{d}m_i}{\mathrm{d}t}-\frac{\mathrm{d}m_\mathrm{d}}{\mathrm{d}t}, \tag{1}$$

where ρ_a is the density of ambient water; Q_e is the entrainment of ambient water; m_i is the mass loss due to dissolution of the oil component i from the buoyant jet/plume into ambient water; and m_d is the mass loss due to turbulent diffusion. The dissolution of oil into water represented by the second term of the right side of Eq. (1) can be calculated by Rye's formulation (1994). Based on Yapa and Zheng's (1997) study, the turbulent diffusion, represented by the third term on the right side of Eq. (1), can be calculated with the concentration gradient.

2.1.2 *Momentum conservation equation*

$$\frac{\mathrm{d}(m\vec{V})}{\mathrm{d}t}=\vec{V}_\mathrm{a}\frac{\mathrm{d}m}{\mathrm{d}t}+m\frac{(\rho_\mathrm{a}-\rho)}{\rho}g\vec{k}, \tag{2}$$

where $\vec{V}_\mathrm{a}$ is the average velocity vector of the ambient current over the exposed buoyant jet/plume surface; and $\vec{k}$ is unit vector in the vertical direction. The first term on the right side of Eq. (2) is the momentum of the entrained mass, and the second term is the force exerted on the CV.

2.1.3 *Heat, salinity and oil mass conservation equation*

Conservation of heat ($C_\mathrm{p}T$), salinity (S), and oil concentration by mass (C) in the CV, are described by (Yapa and Zheng, 1997):

$$\frac{\mathrm{d}(mC_\mathrm{p}T)}{\mathrm{d}t}=C_\mathrm{pa}T_\mathrm{a}\frac{\mathrm{d}m}{\mathrm{d}t}-\rho_\mathrm{a}K_T A\frac{C_\mathrm{p}T-C_\mathrm{pa}T_\mathrm{a}}{b}, \tag{3}$$

$$\frac{\mathrm{d}(mS)}{\mathrm{d}t}=S_\mathrm{a}\frac{\mathrm{d}m}{\mathrm{d}t}-\rho_\mathrm{a}K_S A\frac{S-S_\mathrm{a}}{b}, \tag{4}$$

$$\frac{\mathrm{d}(mC)}{\mathrm{d}t}=C_\mathrm{a}\frac{\mathrm{d}m}{\mathrm{d}t}-\rho_\mathrm{a}K_c A\cdot\frac{C-C_\mathrm{a}}{b}-\sum_i^n\frac{\mathrm{d}m_i}{\mathrm{d}t}-\frac{\mathrm{d}m_\mathrm{d}}{\mathrm{d}t}, \tag{5}$$

where C_p and T are the specific heats and temperature of the oil, respectively; the subscript "a" refers to the ambient water (for oil C_p = 1 800 J/(kg·K) and for water C_pa = 3 900 J/(kg·K)); and K_T, K_S, and K_C are the heat, salinity, and oil concentration diffusivities, respectively ($K_T=2.52\times10^{-4}$ m^2/s, $K_S=1.5\times10^{-9}$m^2/s, and $K_C=1.5\times10^{-9}$m^2/s, Bemporad, 1994).

2.1.4 *State equation*

The density variation of oil due to temperature, salinity and concentration can be described by the state equation. Based on Bemporad's study (1994), the exact functional form for oil is described by

$$\rho=\rho_0\left[1-\beta_T(T-T_0)+\beta_C(C-C_0)\right], \tag{6}$$

where β_T and β_C are the coefficients of heat conduction and dissolution, respectively ($\beta_T=5\times10^{-4}$·°C^{-1} and $\beta_C=8\times10^{-3}$ %$^{-1}$, Bemporad, 1994); and the subscript "0" refers to the initial values.

2.1.5 *Entrainment*

Entrainment of ambient water into the jet/plume, Q_e, in Eq. (1), from both shear-induced entrainment, Q_s, and forced entrainment, Q_f, (Frick, 1984; Lee and Cheung, 1990) is a critical factor in the fate of the jet/plume. The coefficient of shear-induced entrainment can be calculated, based on Schatzmann (1979) and Lee and Cheung's formulations (1990). Furthermore, the modified formulations of forced entrainment were derived by Yapa and Zheng (1997), that were more complete and less complex than those of Lee and Cheung (1990) and Frick (1994). Because of the good agreement between the laboratory and field experiments (Zheng and Yapa, 1998), the same formulation is used here to model the entrainment.

2.1.6 *Particalization of control volume*

The PDM uses the Lagrangian integral CV approach, whereas, the ADM uses the Lagrangian particle method, in which the particle is clearly superior to the CV for describing oil droplets. Therefore, the CV of the present PDM CV needs to be filled with particles to facilitate the butt joint between the PDM and ADM. In the plume-dynamic stage, each particle represents a set of oil droplets of equal size, that is presumed to be a random continuous distribution in the CV. When the CV has reached the transition point, from the PDM to the ADM, all particles are introduced into the ambient, and then move in response to buoyancy, shear current, and turbulence. The particalization processes for the CV are separated into two sub-processes: assignment to the initial coordinates of particles in the CV, and then rotation and translation for the initial coordinates of particles.

First, the equation for assignment to the initial coordinates of particles in the CV can be written as

$$Z\mathrm{d}p=R1(Z(i+die)-Z(i)), \tag{7}$$

$$X\,\mathrm{d}p=[b(i)R2+R1(b(i+die)-b(i))]\times\sin\left(\frac{i}{n}2\pi+\frac{0.1}{n}k\right), \tag{8}$$

$$Y\mathrm{d}p=[b(i)R2+R1(b(i+die)-b(i))]\times\cos\left(\frac{i}{n}2\pi+\frac{0.1}{n}k\right), \tag{9}$$

where $X\,\mathrm{d}p$, $Y\mathrm{d}p$, and $Z\mathrm{d}p$ are the initial coordinates of particles in the x-, y-, and z-directions, respectively; $R1$ and $R2$ are random numbers uniformly distributed in the interval [0, 1]; *die* is the iteration time step; $b(i)$ is the radius at the ith time step; and k is an iteration variable of each set of particles for the CV.

Using the velocity angles of the CV calculated by the PDM, the angle matrix for coordinate rotation (R_0) is then described by

$$R_0 = \begin{pmatrix} \cos\varepsilon_y\cos\varepsilon_z & \cos\varepsilon_y\sin\varepsilon_z & -\sin\varepsilon_y \\ -\cos\varepsilon_x\sin\varepsilon_x+\sin\varepsilon_x\sin\varepsilon_y\cos\varepsilon_z & \cos\varepsilon_x\cos\varepsilon_z+\sin\varepsilon_x\sin\varepsilon_y\sin\varepsilon_z & \sin\varepsilon_x\cos\varepsilon_y \\ \sin\varepsilon_x\sin\varepsilon_z+\cos\varepsilon_x\sin\varepsilon_y\cos\varepsilon_z & -\sin\varepsilon_x\cos\varepsilon_z+\cos\varepsilon_x\sin\varepsilon_y\sin\varepsilon_z & \cos\varepsilon_x\cos\varepsilon_y \end{pmatrix}, \tag{10}$$

where ε_x, ε_y and ε_z are the velocity angles of the CV in the x-, y- and z-directions, respectively.

After rotating the space coordinates by the angle matrix, and then translating to the position of the CV calculated by the PDM, the final discrete particle coordinates can be written as

$$\begin{bmatrix} X_S \\ Y_S \\ Z_S \end{bmatrix} = R_0 \begin{bmatrix} X\,\mathrm{d}p \\ Y\mathrm{d}p \\ Z\mathrm{d}p \end{bmatrix} + \begin{bmatrix} X(i) \\ Y(i) \\ Z(i) \end{bmatrix}, \tag{11}$$

where X_S, Y_S, and Z_S are the final discrete particle coordinates in the x-, y- and z-directions, respectively; and $X(i)$, $Y(i)$ and $Z(i)$ are the coordinates of the CV at the ith time step.

2.2 *Advection-diffusion model*

2.2.1 *Terminal level of plume dynamics*

Based on Rye et al. (1996) and Yapa and Zheng's work (1997) on the transition point from the plume-dynamic stage to the advection-diffusion stage, Dasanayaka and Yapa (2009) studied the various criteria that could be used as the choice of TLPD. Their study suggested that the droplet buoyant velocity, V_b, corresponding to the median oil droplet size based on volume, could be used as the TLPD transition, with the advantage that the model would go directly into the ADM calculation stage when the leak rate, or plume velocity is lower than the buoyancy velocity of the median oil droplet. The droplet buoyant velocity criterion is used in this paper, considering the possibility of slow leaks resulting in immediate advection-diffusion movement.

2.2.2 *Kinematic equation of oil droplets*

The transport of oil moving as individual droplets beyond the buoyant velocity criterion can be calculated by the ADM. The kinematic equation for the displacement vector of a droplet, in a single time step, is described by

$$\vec{S} = \vec{S}_\mathrm{l} + \vec{S}_\mathrm{a} + V_\mathrm{b}\cdot\vec{k}\Delta t, \tag{12}$$

where $\vec{S}_\mathrm{l}$ and $\vec{S}_\mathrm{a}$ are the displacement vectors of droplet due to advection and turbulent diffusion, respectively; V_b is the droplet buoyant velocity; and $\vec{k}$ is unit vector in the vertical direction.

The equation for the displacement vector of a droplet, because of advection, can be written as

$$\vec{S}_\mathrm{l} = \vec{S}_0 + \int_t^{t+\Delta t} \vec{V}_\mathrm{l}(x(t), y(t), t)\mathrm{d}t, \tag{13}$$

where $\vec{S}_0$ is the initial displacement vector of a droplet; and $\vec{V}_\mathrm{l}$ is the velocity vector of the local current.

The equation for the displacement vector of a droplet, due to turbulent diffusion, can be written as

$$\vec{S}_a = \sqrt{6k_a\Delta t}(R_x, R_y, R_z), \tag{14}$$

where k_a is the turbulent diffusion coefficient in x-, y-, and z-directions (for the horizontal diffusivities $k_x = k_y = 0.05$ m^2/s, and for the vertical diffusivity $k_z = 0.001$ m^2/s, Yapa et al., 1999); and R_x, R_y, and R_z are random numbers of normal distribution in the interval [–1, 1].

2.2.3 *Buoyant velocity of oil droplets (V*b*)*

Underwater oil spills contain oil droplets of various sizes, that have different buoyant velocities, V_b, for simulating the fate of oil. Previous studies (e.g., Clift et al., 1978; Takemura and Yabe, 1999) have shown that fluid particles can be spherical (small-size range), ellipsoidal (intermediate-size range), or spherically cap-shaped (large-size range). Based on the studies of Clift et al. (1978), Zheng and Yapa (2000) presented an integrated formulation to compute V_b of bubbles/droplets in the above three size ranges. The same method is used here.

The size distribution of oil droplets from underwater oil spills has a great influence on the fate of oil in the environment (Johansen, 2003; Brandvik et al., 2013). Based on experimental data obtained from oil droplet breakup experiments, conducted in a new test facility at SINTEF, a modified Weber number model for the prediction of droplet size distributions, formed in subsea oil and gas blowouts, was introduced (Johansen et al., 2013). In this model, the same Weber number method is adopted, and the droplet size distribution could then be obtained from the median droplet size, based on the discharge conditions (leak rate, and leak diameter).

3 Model validation

The numerical model developed in Section 2 is tested against a selection of actual experimental data, that includes different discharge and ambient conditions. The experimental conditions used are: slow-discharges in un-stratified stagnant/flowing ambient, given by the China Offshore Oil Engineering Corporation (COOEC); and buoyant jets in both un-stratified flowing ambient and stratified stagnant ambient given by Fan (1967). To differentiate the characteristics of the various experimental conditions, three parameters (Jiang et al., 2016) are introduced:

$$Fr_0 = \frac{\left|\vec{V}\right|}{\sqrt{g'_0 D}}, \tag{15}$$

$$St_0 = \frac{\Delta\rho_0}{D\left.\dfrac{\mathrm{d}\rho_\mathrm{a}}{\mathrm{d}z}\right|_{z=0}}, \tag{16}$$

$$R_0 = \frac{\left|\vec{V}\right|}{\left|\vec{V}_a\right|}, \tag{17}$$

in which the subscript "0" refers to initial values; Fr is the jet densimetric Froude number; $g' = g(\rho_a - \rho/\rho)$; D is the diameter of orifice, i.e., leak diameter; St is the stratification number; R is the ratio between the magnitudes of the jet and cross-flow velocities; and ϕ_0 is the angle between the discharge direction and the positive direction of the x-axis. The values of the primary parameters used in the experiments are presented in Table 1, and other specific parameters are detailed in the section below.

Table 1. Primary experimental parameters

Description	No.	Author	Fr_0	St_0	R_0	$\phi_0/(°)$
Slow-discharges in unstratified flowing ambient	FC-0	COOEC	1.975	∞	∞	90.0
	FC-1		1.975	∞	4.618	90.0
	FC-2		1.975	∞	2.506	90.0
	FC-3		1.975	∞	1.667	90.0
	FC-4		1.975	∞	1.245	90.0
Buoyant jets in unstratified flowing ambient	FF-1	Fan (1967)	20.000	∞	4.000	90.0
	FF-2		20.000	∞	8.000	90.0
	FF-3		18.479	∞	12.048	90.0
Buoyant jets in stratified stagnant ambient	FF-4		36.000	212	∞	45.0
	FF-5		20.000	107	∞	39.1
	FF-6		13.000	113	∞	2.8

3.1 *Experiments from COOEC*

To validate the accuracy of the oil spill model for simulating slow leaks with simple ADM, the COOEC series experiments were run by the authors at the Tianjin Research Institute for Water Transport Engineering, using a water tank 0.7 m long, 0.5 m wide and 0.5 m deep. As shown in Fig. 2, an oil pipe was buried at the bottom of the test tank along the flow direction. A round hole, with a diameter of 4 mm, was opened on top of the pipe to mimic the pipe leaks. A camera was positioned on one side of tank to record the oil spill process. According to the different current conditions, a total of five density un-stratified experiments were selected to calibrate the numerical model in this section. The fixed experimental parameters are presented in Table 2, and Fig. 3 shows the unidirectionally non-uniform current profiles corresponding to FC-1 through FC-4.

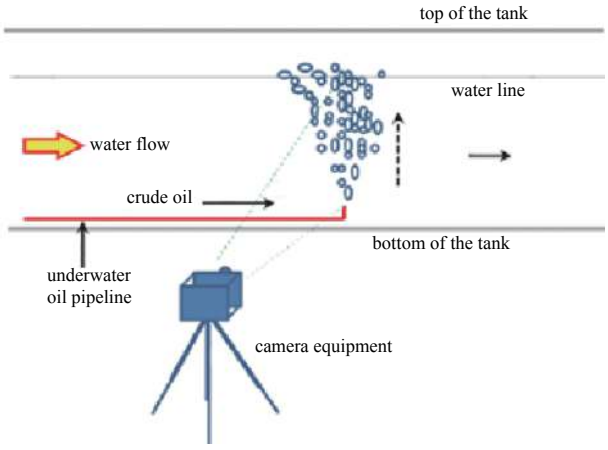

Fig. 2. COOEC experimental setup.

Model validation entails detailed comparisons of model simulations with photographic observations, that include the trajectory of the spilled oil, the leakage time, and the maximum lateral migration distance when the oil reaches the sea surface. Figure 4 shows the trajectory comparisons, for FC-0, FC-1, FC-2, FC-3 and FC-4, with the model calculations. It can be seen that the CFD oil trajectory simulations in the water were in a good agreement with the experimental data. The detailed comparison of the leakage time and the maximum lateral migration distance is presented in Table 3. The numerical results agree well with the experimental results, except for a marginal underestimation of the leakage time observed in simulations.

Table 2. Fixed experimental parameters

Specific parameters	Value
Oil density/kg · m^{-3}	894.900
Water density/kg · m^{-3}	983.300
Oil viscosity/mPa · s	284.200
Oil temperature/°C	53.000
Water temperature/°C	24.000
Leakage rate/m · s^{-1}	0.123
Leak diameter/m	0.004
Water depth/m	0.500

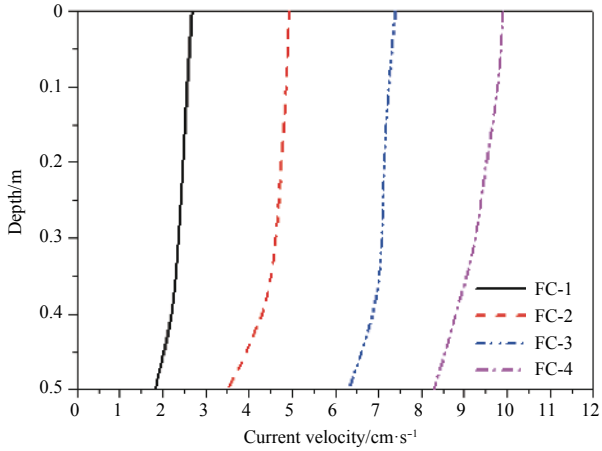

Fig. 3. Current velocity profiles of COOEC series tests.

3.2 *Experiments from Fan (1967)*

Two types of experiments by Fan (1967) were selected to further validate the accuracy of the model for simulating buoyant jets/plumes with combinations of PDM and ADM, and were identified as FF-1, FF-2, and FF-3 and FF-4, FF-5 and FF-6. The experiments were conducted in a laboratory tank, filled with

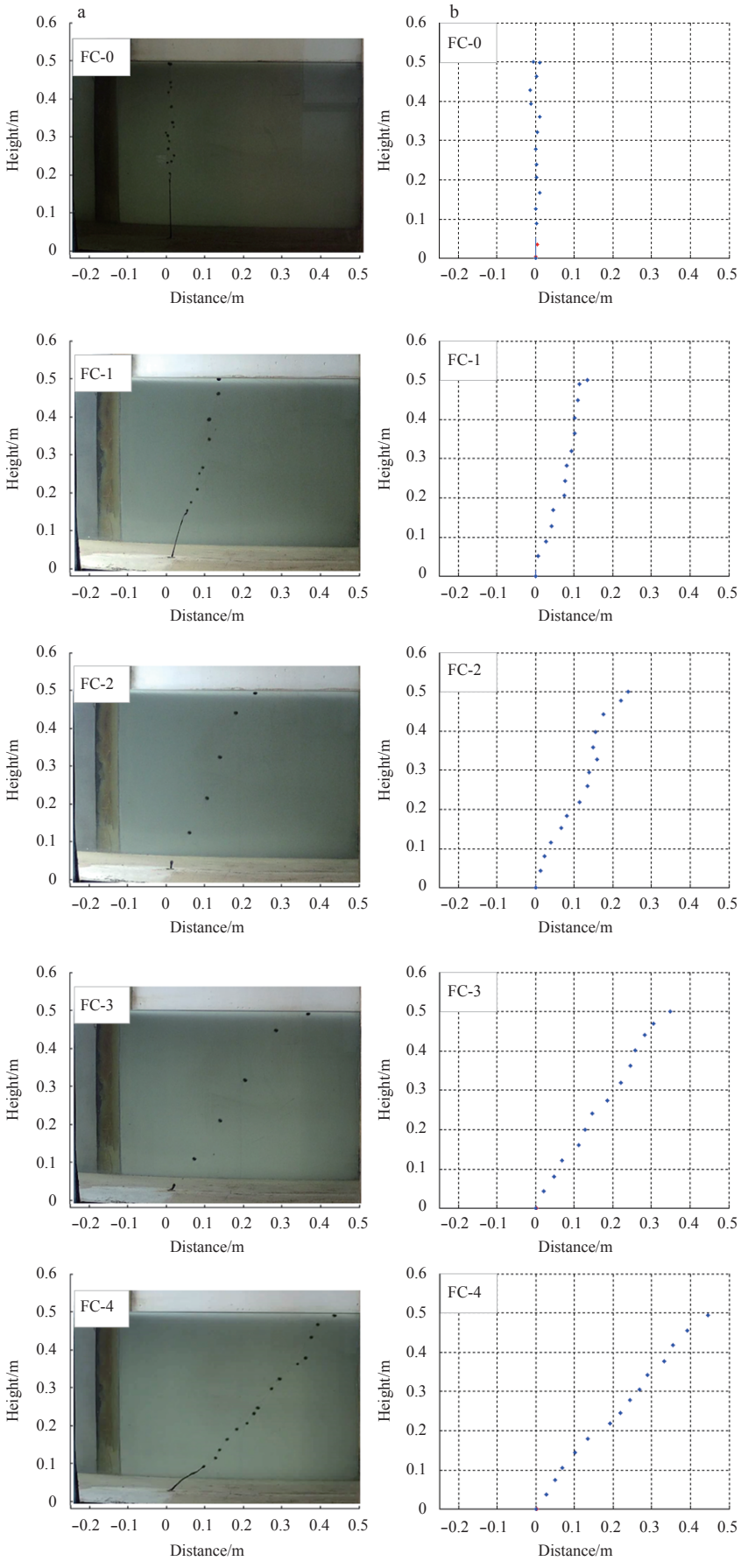

Fig. 4. Comparisons of trajectories for FC-0, FC-1, FC-2, FC-3 and FC-4 with model calculations. a. Experiment, b. simulation.

Table 3. Experimental and numerical results for selected cases

No.	Experimental lateral migration distance/m	Numerical lateral migration distance/m	Relative error/%	Experimental leakage time/s	Numerical leakage time/s	Relative error/%
FC-0	0.005	0.005	11.1	5.04	5.03	–0.2
FC-1	0.136	0.142	4.4	5.08	5.01	–1.4
FC-2	0.233	0.240	3.0	5.56	5.26	–5.4
FC-3	0.366	0.354	–3.3	5.44	4.90	–9.9
FC-4	0.443	0.441	–0.5	5.00	4.89	–2.2

density un-stratified flowing fluid (FF-1, FF-2 and FF-3), and linearly density stratified stagnant fluid (FF-4, FF-5, and FF-6) modeled by filling, layer by layer, with salt solutions of different densities. The current for FF-1, FF-2 and FF-3 was unidirectionally uniform. The diameters of the orifices were 0.76 cm (FF-1, FF-2 and FF-3), and 0.46 cm (FF-4, FF-5 and FF-6). The discharge and ambient characteristics corresponding to the simulated cases were input based on the experimental data, that was detailed in the laboratory report prepared by Fan (1967). Figures 5 and 6 show the comparison between the computed trajectories and the experimental data. Figure 5 shows the density un-stratified flowing fluid, and Fig. 6 shows the linearly density-stratified stagnant fluid. The overall simulation is in satisfactorily good agreement with the experimental data.

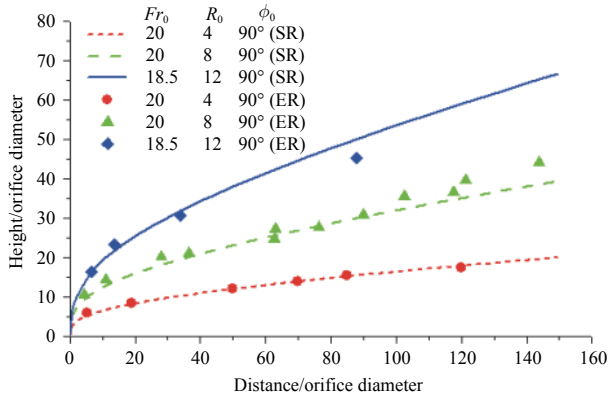

Fig. 5. Comparison of the trajectories for buoyant jets discharged vertically to un-stratified flowing ambient (FF-1, FF-2 and FF-3) between experimental results (ER) and simulation results (SR).

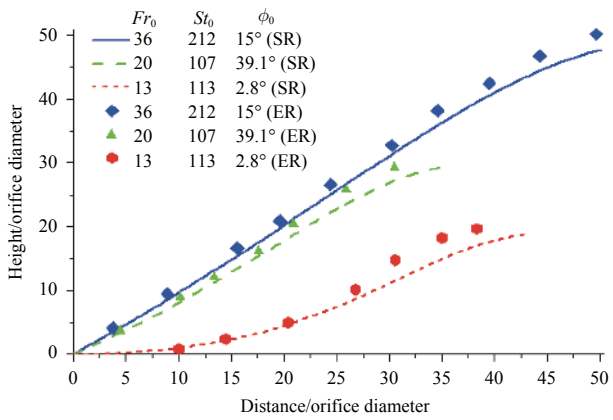

Fig. 6. Comparison of the trajectories for buoyant jets discharged to stratified stagnant ambient (FF-4, FF-5 and FF-6) between experimental results (ER) and simulation results (SR).

4 Parametric study

In the parametric study, 13 hypothetical cases are developed to mimic probable underwater releases in a stratified environment, with a water depth H of 16 m. The ambient temperature and salinity are set as 10°C and 34 at the seabed, and 12°C and 30 at the surface, in order to consider the stratification. The oil temperature, oil viscosity, and ambient density, ρ_a, at the orifice are set as 30°C, 284.2 mPa · s, and 1 027.6 kg/m^3, respectively. The unidirectional current velocities are assumed to have logarithmic profiles: $V_a = k_a \times \log(1+z)$ [m/s], where the current velocity at the surface, V_{amax} is $k_a \times \log(1+16)$. The value of k_a falls in the range 0.081–0.203.

As shown in Table 4, the oil density, current velocity at the surface, leak rate, and leak diameter are varied from case to case. As the leak rate and leak diameter are interrelated, the minimum volume flux in Case 8 (leak rate 0.5 m/s, and leak diameter 0.06 m) has been set as a comparison standard for others cases, as presented in Table 4. Therefore, a certain range of volume flux of leaking oil has been considered in this section.

The simulation results of the underwater oil spread process are shown in Figs 7–10. Spilled oil first rises as a jet/plume, losing momentum and buoyancy gradually because of the entrainment of the stratified ambient fluid, i.e., the plume-dynamic stage. Beyond the terminal level of plume dynamics, the plume cloud is broken up into individual droplets affected by advection and diffusion, i.e., advection-diffusion stage. Under the action of shear current, oil droplets become more dispersed with increasing height. To facilitate the analysis of the oil spill process, the plume-dynamic and advection-diffusion stages are depicted by red and blue, respectively. We adopt Case 2 (as shown in Table 4) as the standard case.

4.1 *Effect of oil density*

To study the effect of oil density, simulations are conducted by changing the oil density while keeping other parameters the same as those in the standard case. Figure 7 shows the process of oil spills from pipelines to the sea surface for four different oil densities. It is observed that the leakage time, the lateral migration distance, and the surface diffusion range increase with increasing oil density. The leakage time, and lateral migration distance, of heavy oil ($\rho_0 = 930$ kg/m^3) are approximately 1.36 times and 1.55 times greater than those at a density of 780 kg/m^3, respectively. Moreover, the diffusion range of heavy oil is 16.7 m, approximately 2.13 times greater than the 7.83 m with an oil density of 780 kg/m^3. The primary cause of this is that high density oil droplets rise slower, because of the effect of gravity, leading to both a longer underwater action time and longer plume-dynamic stage. Based on the strong active diffusion of a buoyant plume relative to the advection-diffusion stage, a longer plume-dynamic stage results in a greater surface diffusion range. The lateral migration distance also increases with increasing flow action time.

Table 4. Simulation cases

Case	Oil density (ρ_0)/kg/m^{-3}	Current velocity at surface (V_{amax})/m · s^{-1}	Leak rate (V_0)/m · s^{-1}	Leak diameter (D)/m	Volume flux of leaking oil/m^3 · s^{-1}	Flux multiple (compared with Case 8)
1	780	0.15	1.0	0.06	0.002 827	2.0
2	830	0.15	1.0	0.06	0.002 827	2.0
3	880	0.15	1.0	0.06	0.002 827	2.0
4	930	0.15	1.0	0.06	0.002 827	2.0
5	830	0.10	1.0	0.06	0.002 827	2.0
6	830	0.20	1.0	0.06	0.002 827	2.0
7	830	0.25	1.0	0.06	0.002 827	2.0
8	830	0.15	0.5	0.06	0.001 414	1.0
9	830	0.15	1.5	0.06	0.004 241	3.0
10	830	0.15	2.0	0.06	0.005 655	4.0
11	830	0.15	1.0	0.05	0.001 963	1.4
12	830	0.15	1.0	0.07	0.003 848	2.7
13	830	0.15	1.0	0.08	0.005 027	3.6

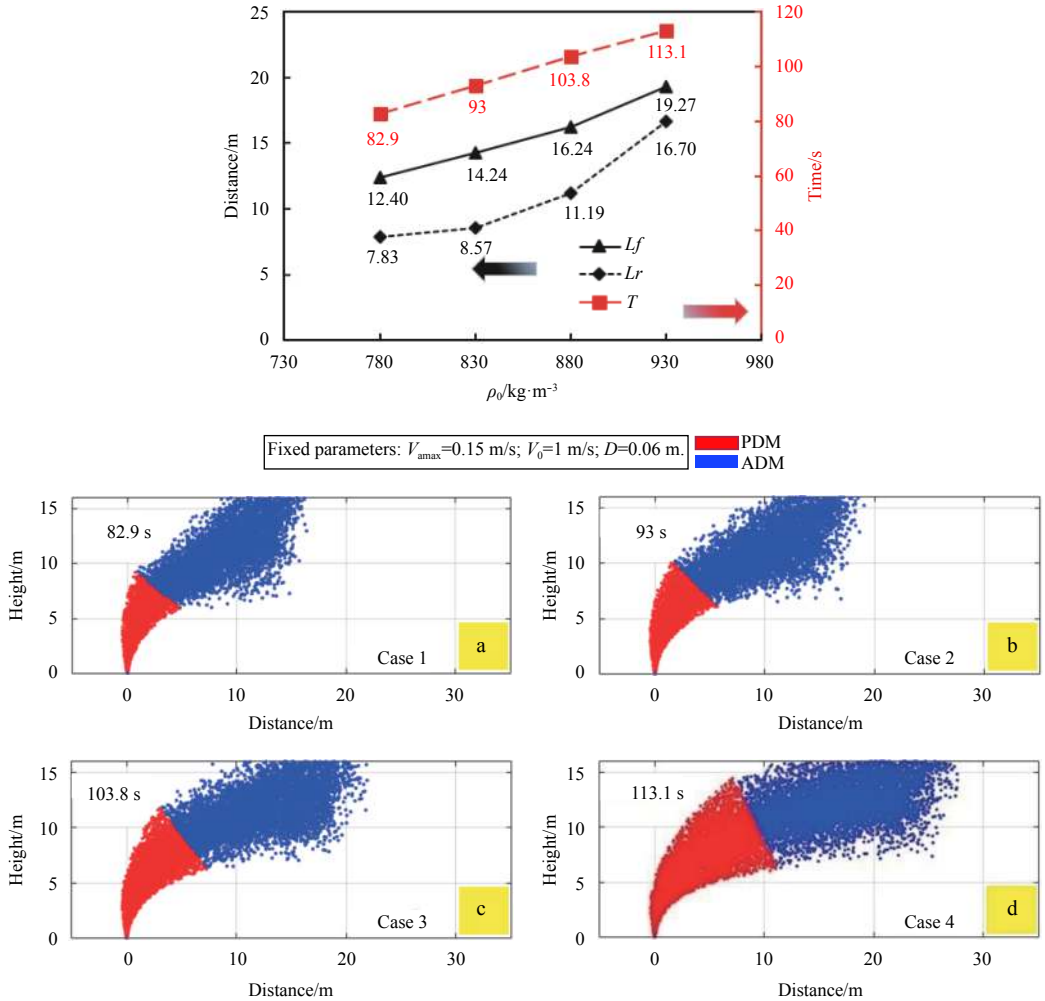

Fig. 7. Leakage time (T), lateral migration distance (Lf), surface diffusion range (Lr), and underwater spread of spilled oil at different oil densities: $\rho_0 = 780$ kg/m^3 (a); $\rho_0 = 830$ kg/m^3 (b); $\rho_0 = 880$ kg/m^3 (c); and $\rho_0 = 930$ kg/m^3 (d).

4.2 *Effect of current velocity*

The process of oil spilling from a pipeline at four different current velocities is shown in Fig. 8. It can be seen that the greater the current velocity, the greater the horizontal trajectory of the spilled oil. Current as a carrier plays a critical role in the entrainment (jet/plume) and lateral action of spilled oil. The process of the ambient water entering the plume is accelerated by the entrainment of rapid current, that could reduce the rising momentum of the plume cloud, and increase the lateral movement. Therefore, the leakage time, the lateral migration distance, and

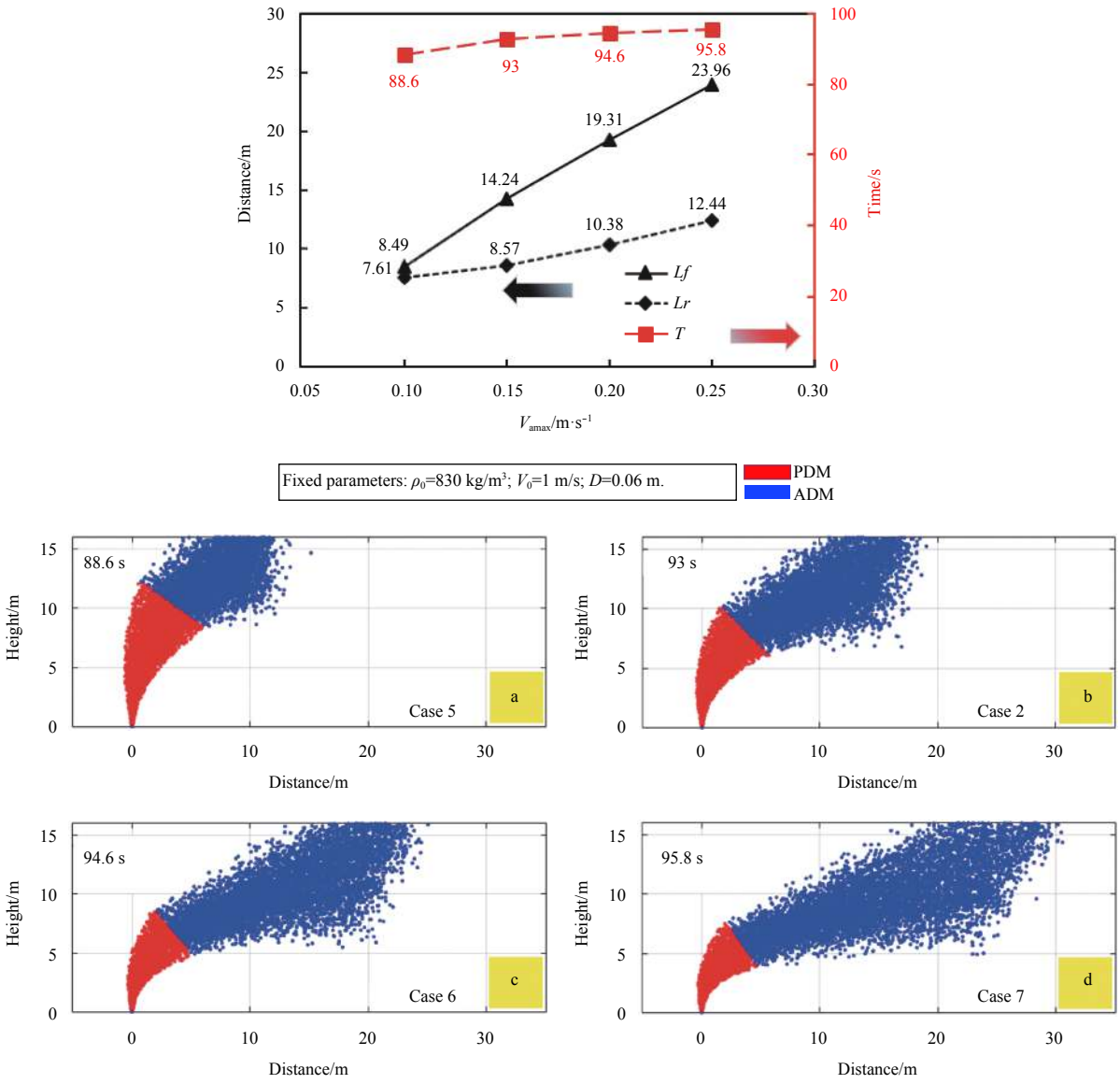

Fig. 8. Leakage time (T), lateral migration distance (Lf), surface diffusion range (Lr), and underwater spread of spilled oil at different current velocities: a. $V_{a\,max}$ = 0.1 m/s; b. $V_{a\,max}$ = 0.15 m/s; c. $V_{a\,max}$ = 0.2 m/s; d. $V_{a\,max}$ = 0.25 m/s.

the surface diffusion range all increase with increasing current velocity. As the current velocity increases from 0.1 m/s to 0.25 m/s, the leakage time, the lateral migration distance, and the diffusion range increase by 8.13%, 182.2% and 63.5%, respectively. In particular, the effect of current on the lateral migration distance is clearly evident.

4.3 *Effect of leaking flux*

The volume flux of spilled oil is primarily determined by the leak size, and the leak rate. Figure 9 shows the underwater spreading process of spilled oil for four different leak rates, with a leak diameter of 0.06 m. It can be seen that the arrival time, and the lateral migration distance, decrease with increasing leak rates, while the surface diffusion range exhibits the opposite trend. Because of the high buoyant kinetic energy of the plume, the oil spilled at a greater leak rate rises and spreads faster, resulting in both a greater leakage time and lateral migration distance. Therefore, as the leak rate increases from 0.5 m/s to 2 m/s, the leakage time decreases by 26.8%, and the diffusion range increases by 136%. With a leak rate from 0.5–1 m/s, the diffusion range increases marginally, but increases rapidly when the leak rate changes from 1–2 m/s. Primarily because of the long current action, the lateral migration distance for V_0 = 0.5 m/s is 14.63 m, approximately 1.15 times greater than that for V_0 = 2 m/s.

In addition to the leak rate, the leak diameter is also considered in this study. Figure 10 shows the underwater spread process of spilled oil from four different leak diameters, at the same leak rate V_o = 1 m/s. It can be seen that greater leak diameters result in shorter arrival times, smaller lateral migration distances, and greater surface diffusion ranges. The mechanism of the spread process is similar to the cases with different leak rates. As the leak diameter increases from 0.05–0.08 m, the leakage time and the lateral migration distance decrease by 24.2% and 30.5%, respectively. Moreover, the diffusion range for D = 0.05 m is 7.1 m, that is approximately 56% of that for D = 0.08 m.

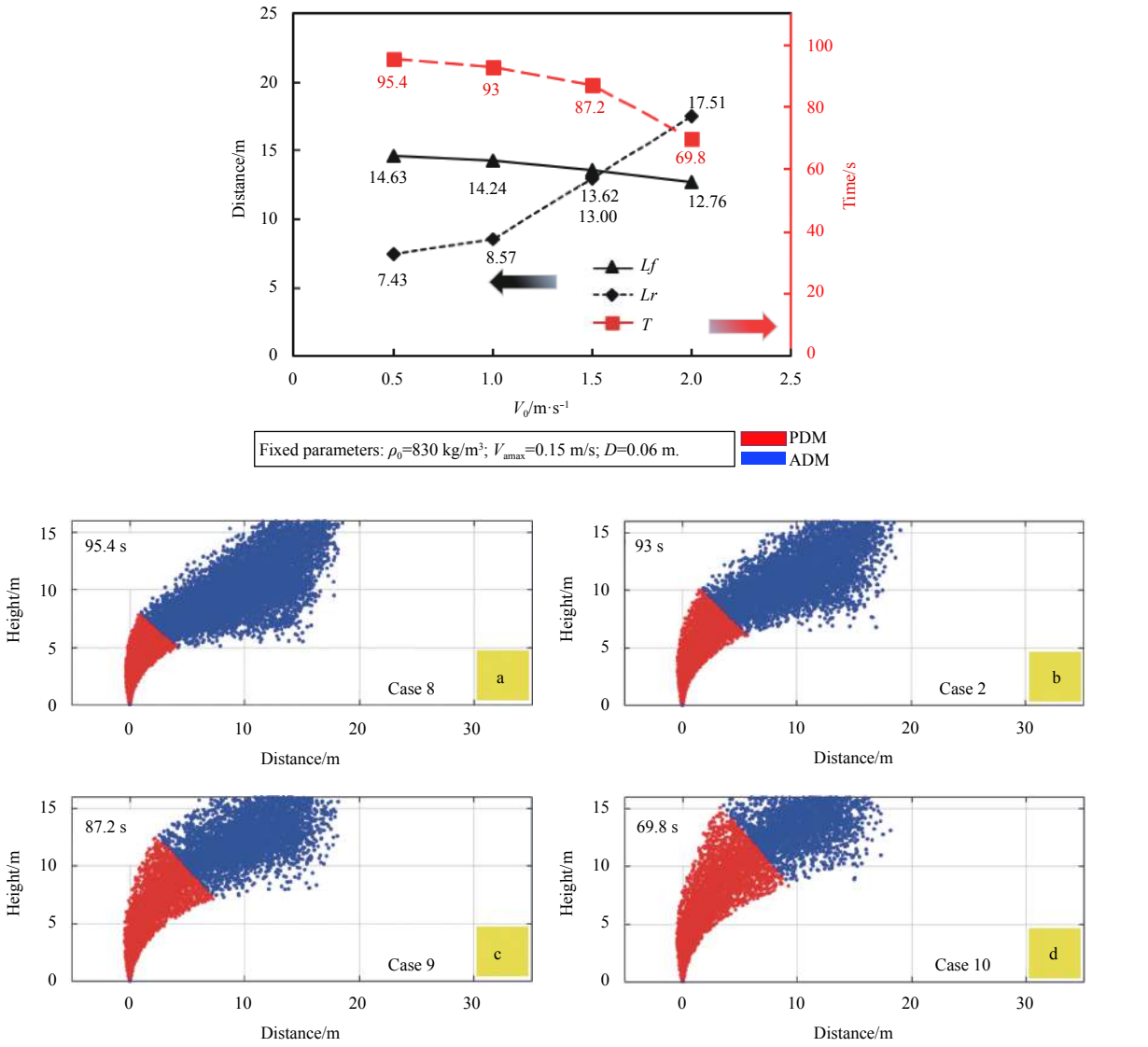

Fig. 9. Leakage time (T), lateral migration distance (Lf), surface diffusion range (Lr), and underwater spread of spilled oil at different leak rates: $V_o = 0.5$ m/s (a); $V_o = 1$ m/s (b); $V_o = 1.5$ m/s (c); and $V_o = 2$ m/s (d).

5 Conclusions

In this study, a numerical model was developed to simulate underwater oil spills. The numerical model comprised two sub-models: the PDM was based on the Lagrangian integral method, while the ADM was based on the Lagrangian particle method. The model can take into account not only the unsteady nature of currents, and the diffusion and dissolution of oil, but also the density stratification of the ambient water. The particalization of the control volume is conducted so that comprehensive, and successive, simulations on oil spill fate can be performed. The oil spill process can be simulated from the seabed to the sea surface, predicting when and where the oil will reach the sea surface. The model is capable of a fast，real-time and accurate prediction of oil spills, spreads that originate as jets/plumes, and slow leaks. Therefore, the model is a useful tool for early emergency response to unexpected oil spills.

For verifying the applicability, the model was tested against a selection of actual experimental data from COOEC and Fan (1967), that includes different discharge and ambient conditions. In all cases, the comparisons have been reasonably good. The trajectory of spilled oil, the leakage time, and the maximum lateral migration distance when oil reaches the sea surface of the model, were in good agreement with the experimental data. Compared to the COOEC slow leak experimental data, the numerical model predicted a shorter arrival time at the free surface. In certain circumstances, this could be attributed to the boundary limitations in the scaled experiment. Therefore, the verified model can provide a satisfactory technical reference for oil spill response.

Finally, the effects of oil density, current velocity, leak rate, and leak diameter were examined by the validated CFD model. It was observed that the greater the density of the oil, the faster the current and the slower the oil leak, or the smaller the leak diameter, the greater both the leakage time and lateral migration distance. The surface diffusion range increased with increasing oil density, current velocity, leak rate and leak diameter. In particular, the effect of current on the lateral migration distance and that of the leak rate on surface diffusion range were more evident. Although the results were obtained under specific conditions, they can provide practical predictions and useful guidance

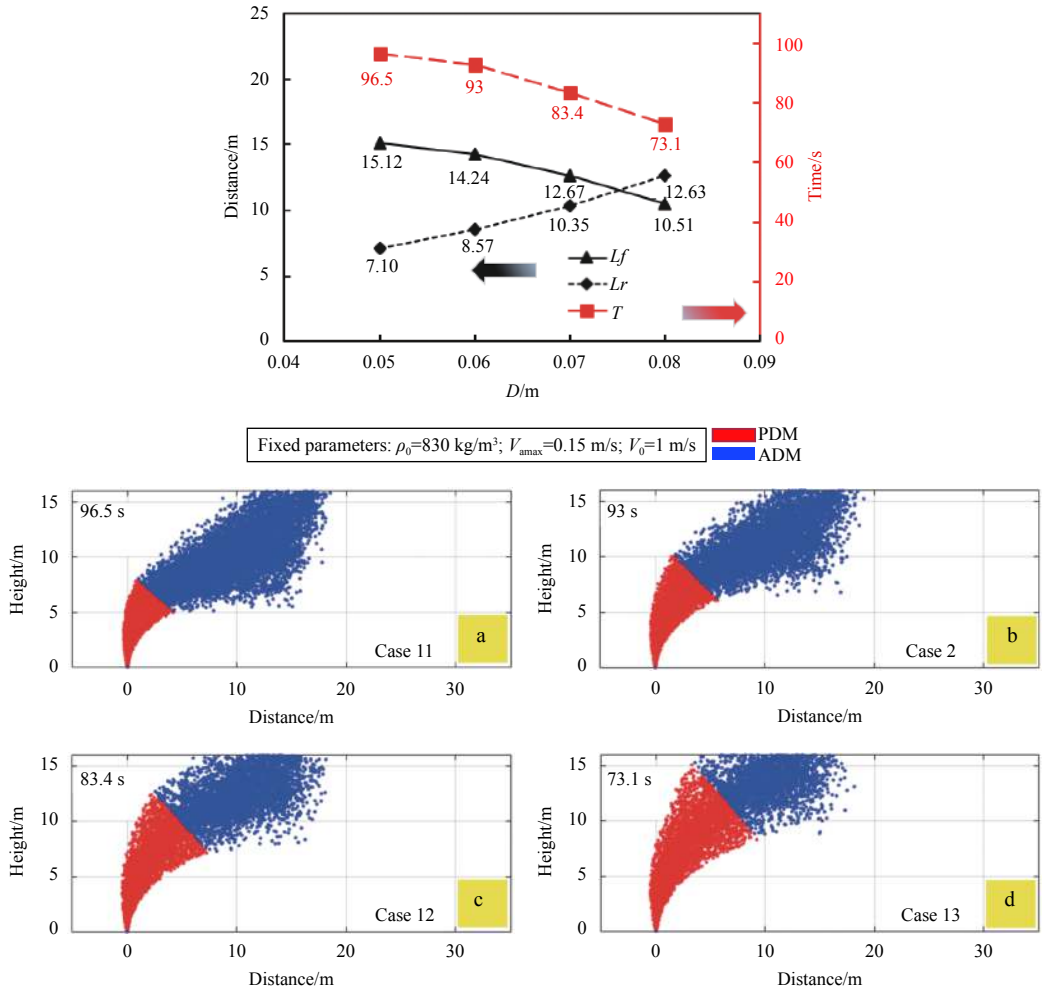

Fig. 10. Leakage time (T), lateral migration distance (Lf), surface diffusion range (Lr), and underwater spread of spilled oil at different leak diameters: $D = 0.05$ m (a); $D = 0.06$ m (b); $D = 0.07$ m (c); and $D = 0.08$ m (d).

for emergency rescues during an accidental spill.

With significant oil exploration and production activity taking place in significantly deeper waters, as well as the absence of experimental evidence as to when the plume dynamics cease to exist in a plume cloud, future studies should concentrate on the understanding and modeling of the physical-chemical processes of deepwater oil spills in high-pressure and low-temperature environments, as well as experimental studies on the TLPD.

Acknowledgments

The authors thank the COOEC water tank experiments for the experimental data support.

References

ASCE Task Committee on Modeling of Oil Spills. 1996. State-of-the-art Review of modeling transport and fate of oil spills. Journal of Hydraulic Engineering, 122(11): 594–609, doi: 10.1061/(ASCE)0733-9429(1996)122:11(594)

Bemporad G A. 1994. Simulation of round buoyant jet in stratified flowing environment. Journal of Hydraulic Engineering, 120(5): 529–543, doi: 10.1061/(ASCE)0733-9429(1994)120:5(529)

Boufadel M C, Abdollahi-Nasab A, Geng X L, et al. 2014. Simulation of the landfall of the deepwater horizon oil on the shorelines of the Gulf of Mexico. Environmental Science & Technology, 48(16): 9496–9505

Brandvik P J, Johansen Ø, Leirvik F, et al. 2013. Droplet breakup in subsurface oil releases - Part 1: Experimental study of droplet breakup and effectiveness of dispersant injection. Marine Pollution Bulletin, 73(1): 319–326, doi: 10.1016/j.marpolbul.2013.05.020

Chen Haibo, An Wei, You Yunxiang, et al. 2015. Numerical study of underwater fate of oil spilled from deepwater blowout. Ocean Engineering, 110: 227–243, doi: 10.1016/j.oceaneng.2015.10.025

Clift R, Grace J R, Weber M E. 1978. Bubbles, Drops, and Particles. New York: Academic Press

Dasanayaka L K, Yapa P D. 2009. Role of plume dynamics phase in a deepwater oil and gas release model. Journal of Hydro-environment Research, 2(4): 243–253, doi: 10.1016/j.jher.2009.01.004

Deng Zengan, Yu Ting, Jiang Xiaoyi, et al. 2013. Bohai Sea oil spill model: a numerical case study. Marine Geo-physical Research, 34(2): 115–125, doi: 10.1007/s11001-013-9180-x

Fan L N. 1967. Turbulent buoyant jets into stratified or flowing ambient fluids. Pasadena, Calif: W M Keck Labor-atory for Hydraulics and Water Resources, California Institute of Technology

Fannelop T K, Sjoen K. 1980. Hydrodynamics of underwater blowouts. In: AIAA 8th Aerospace Sciences Meeting. Pasadena, California: AIAA

Fanneløp T K, Hirschberg S, Küffer J. 1991. Surface current and recirculating cells generated by bubble curtains and jets. Journal of Fluid Mechanics, 229(1): 629–657

Frick W E. 1984. Non-empirical closure of the plume equations. Atmospheric Environment (1967), 18(4): 653–662, doi: 10.1016/0004-6981(84)90252-X

Frick W E. 1994. A Lagrangian philosophy for plume modeling [dis-

sertation]. Southampton: Oregon State University
Hackett B, Comerma E, Daniel P, et al. 2009. Marine oil pollution prediction. Oceanography, 22(3): 168–175, doi: 10.5670/oceanog
Jiang Meirong, Li Zhigang, Yu Jianxing. 2016. Effect of grid density on numerical result for oil leakage from subsea pipeline. Journal of Tianjin University (Science and Technology) (in Chinese), 49(9): 907–914
Johansen Ø. 2000. *DeepBlow* - a Lagrangian plume model for deep water blowouts. Spill Science & Technology Bulletin, 6(2): 103–111
Johansen Ø. 2003. Development and verification of deep-water blowout models. Marine Pollution Bulletin, 47(9-12): 360–368, doi: 10.1016/S0025-326X(03)00202-9
Johansen Ø, Brandvik P J, Farooq U. 2013. Droplet breakup in subsea oil releases - Part 2: Predictions of droplet size distributions with and without injection of chemical dispersants. Marine Pollution Bulletin, 73(1): 327–335, doi: 10.1016/j.marpolbul.2013.04.012
Lee J H W, Cheung V. 1990. Generalized Lagrangian model for buoyant jets in current. Journal of Environmental Engineering, 116(6): 1085–1106, doi: 10.1061/(ASCE)0733-9372(1990)116:6(1085)
Li Wei, Pang Yongjie, Lin Jianguo, et al. 2013. Computational modeling of submarine oil spill with current and wave by FLUENT. Research Journal of Applied Sciences, Engineering and Technology, 5(21): 5077–5082, doi: 10.19026/rjaset.5.4400
Marta-Almeida M, Ruiz-Villarreal M, Pereira J, et al. 2013. Efficient tools for marine operational forecast and oil spill tracking. Marine Pollution Bulletin, 71(1–2): 139–151, doi: 10.1016/j.marpolbul.2013.03.022
McDougall T J. 1978. Bubble plumes in stratified environments. Journal of Fluid Mechanics, 85(4): 655–672, doi: 10.1017/S0022112078000841
Milgram J H. 1983. Mean flow in round bubble plumes. Journal of Fluid Mechanics, 133(1): 345–376
Paiva P M, Lugon J J, Barreto A N, et al. 2017. Comparing 3d and 2d computational modeling of an oil well blowout using MOHID platform - A case study in the Campos Basin. Science of the Total Environment, 595: 633–641, doi: 10.1016/j.scitotenv.2017.04.007
Rye H. 1994. Model for calculation of underwater blow-out plume. Proceedings of the Seventeenth Arctic and Marine Oil Spill Program (AMOP) Technical Seminar, 2: 849–865
Rye H, Brandvik P J. 1997. Verification of subsurface oil spill models. In: Proceedings of the 1997 International Oil Spill Program Conference. Fort Lauderdale, Florida: IOSC, 551–577
Rye H, Brandvik P J, Reed M. 1996. Subsurface oil release field experiment-observations and modeling of subsur-face plume behavior. Proceedings of the Nineteenth Arctic and Marine Oil Spill Program (AMOP) Technical Seminar, 2(1): 1417–1435
Schatzmann M. 1979. An integral model of plume rise. Atmospheric Environment (1967), 13(5): 721–731, doi: 10.1016/0004-6981(79)90202-6
Spaulding M L. 2017. State of the art review and future directions in oil spill modeling. Marine Pollution Bulletin, 115(1–2): 7–19, doi: 10.1016/j.marpolbul.2017.01.001
Takemura F, Yabe A. 1999. Rising speed and dissolution rate of a carbon dioxide bubble in slightly contaminated water. Journal of Fluid Mechanics, 378(1): 319–334
Tangley L. 2010. Oil spill hammers brown pelicans. National Wildlife, 48(6): 12
Wang Chuanyuan, Chen Bing, Zhang Baiyu, et al. 2013. Fingerprint and weathering characteristics of crude oils after Dalian oil spill, China. Marine Pollution Bulletin, 71(1–2): 64–68, doi: 10.1016/j.marpolbul.2013.03.034
Xu Qing, Li Xiaofeng, Wei Yongliang, et al. 2013. Satellite observations and modeling of oil spill trajectories in the Bohai Sea. Marine Pollution Bulletin, 71(1–2): 107–116, doi: 10.1016/j.marpolbul.2013.03.028
Yang Yiqiu, Li Yan, Liu Guimei, et al. 2017. A hindcast of the Bohai Bay oil spill during June to August 2011. Acta Oceanologica Sinica, 36(11): 21–26, doi: 10.1007/s13131-017-1135-7
Yapa P D, Wimalaratne M R, Dissanayake A L, et al. 2012. How does oil and gas behave when released in deep-water? Journal of Hydro-Environment Research, 6(4): 275–285, doi: 10.1016/j.jher.2012.05.002
Yapa P D, Zheng Li. 1997. Simulation of oil spills from underwater accidents I: Model development. Journal of Hydraulic Research, 35(5): 673–688, doi: 10.1080/00221689709498401
Yapa P D, Zheng Li, Nakata K. 1999. Modeling underwater oil/gas jets and plumes. Journal of Hydraulic Engi-neering, 125(5): 481–491, doi: 10.1061/(ASCE)0733-9429(1999)125:5(481)
Zhang Jun, Zang Xiaogang, Zhang Yuanchun, et al. 2016. Dynamic characteristics of plume/jet from underwater pipe downward leakage. CIESC Journal (in Chinese), 67(12): 4969–4975
Zheng Li, Yapa P D. 1998. Simulation of oil spills from underwater accidents II: Model verification. Journal of Hydraulic Research, 36(1): 117–134, doi: 10.1080/00221689809498381
Zheng Li, Yapa P D. 2000. Buoyant velocity of spherical and non-spherical bubbles/droplets. Journal of Hydraulic Engineering, 126(11): 852–854, doi: 10.1061/(ASCE)0733-9429(2000)126:11(852)
Zheng Li, Yapa P D, Chen Fanghui. 2003. A model for simulating deepwater oil and gas blowouts-PartI: Theory and model formulation. Journal of Hydraulic Research, 41(4): 339–351, doi: 10.1080/00221680309499980
Zheng Quanan, Zhao Qing, Nan W, et al. 2010. Oil spill in the Gulf of Mexico and spiral vortex. Acta Oceanologica Sinica, 29(4): 1–2, doi: 10.1007/s13131-010-0044-9
Zhu Hongjun, Lin Pengzhi, Pan Qian. 2014. A CFD (computational fluid dynamic) simulation for oil leakage from damaged submarine pipeline. Energy, 64: 887–899, doi: 10.1016/j.energy.2013.10.037
Zhu Hongjun, You Jiahui, Zhao Honglei. 2017. Underwater spreading and surface drifting of oil spilled from a submarine pipeline under the combined action of wave and current. Applied Ocean Research, 64: 217–235, doi: 10.1016/j.apor.2017.03.007